SUPPLEMENTARY MATERIAL

Metal Ions Stabilize a Dimeric Molten Globule State Between the Open- and Closed-Forms of Malic Enzyme

Hui-Chuan Chang, Liang-Yu Chen, Yi-Hang Lu, Meng-Ying Li, Yu-Hou Chen, Chao-Hsiung Lin, and Gu-Gang Chang

Department of Life Sciences and Institute of Genome Sciences
National Yang-Ming University, Taipei 112, Taiwan

MATERIALS AND METHODS

Expression and Purification of the Recombinant Malic Enzymes

The recombinant DNA (PET-21-ME) plasmid was transformed into the *E. coli* BL21 bacterial strain and the culture allowed to grow at 37 °C to reach an A_{600} of 0.6-0.8. Enzyme synthesis was then induced by addition of 1 mM isopropyl β-D-thiogalactopyranoside. The cells were incubated at 25 °C for additional 20-h and then harvested by centrifugation at 5000 x g for 10-min. The resuspended cells were sonicated in 30 mM Tris-acetate buffer containing 2 mM 2-mercaptoethanol (pH 7.4) and the recombinant enzyme was purified to apparent homogeneity by Q-Sepharose and adenosine-2',5'-bisphosphate-agarose chromatography as described previously (14). The purified enzyme was subjected to SDS/PAGE to assess purity (Fig. 1S).

Amino Acid Sequence Analysis

SDS-PAGE was carried out in 4-12% pre-cast gradient gel (QIAGENE) and 2-(N-morpholino)-ethanesulfonic acid (MES) running buffer. Proteins were transferred from the gel to polyvinylidene difluoride (PVDF) membrane and stained with Coomassie blue for 2-min. The target protein bands was then cut out from the PVDF membrane and subjected to amino acid sequence analysis using the automated Edman degradation method in a PROCISE 492 protein sequencer (Applied Biosystems).

Mass Spectral Analysis

The matrix of 2,4-dimethoxy-3-hydroxycinnamic acid (sinapinic acid, SA) were obtained from Bruker Daltonics and used without further purification. All mass spectra were acquired on a MALDI-TOF MS (Ultraflex, Bruker Daltonics) equipped with a gridless delayed extraction ion source, a nitrogen laser, a low-mass ion suppressor, a precursor ion selector, a collision cell, a LIFT cell for fragment ion post acceleration, and a gridless ion reflector.

Enzyme samples were dissolved in 50% acetonitrile/0.1% TFA and mixed with matrix solution (10 mg/ml of SA in 50% acetonitrile/0.1% TFA) in 1:1 ratio. Two-microliter aliquots of the resulted protein/matrix mixtures were applied to a stainless steel target plate for subsequent analysis.

MS spectra from intact protein samples were recorded in positive linear mode using 20-kV acceleration voltage, 550-ns ion extraction delay, 1.3-kV detector gain, and 100-mV digitizer sensitivity. The low-mass ion deflector cutoff was set to 10 kDa. The laser power level was raised ~60% beyond the threshold in linear mode. The TOF analyzer was externally calibrated in linear mode using protein standards (Bruker protein calibration kit) before the spectra were collected. All the MS spectra resulted from the accumulation of at least 150 laser shots. Protein masses were determined using FlexAnalysis 2.0 (Bruker Daltonics) with manual peak picking.

Enzyme Assay

Malic enzyme activity was assayed according to the published procedure (14). A 1-ml reaction mixture contained 66.7 mM triethanolamine/HCl buffer (pH 7.4), 5 mM malate, 0.23 mM $NADP^+$, 4 mM Mn^{2+}, and an appropriate amount of enzyme. The formation of NADPH at 30 °C was monitored continuously at 340 nm with a Jasco V550 spectrophotometer.

TABLE 1S
The synthetic oligonucleotides used as mutagenic primers for wild type and tryptophanyl mutants of pigeon c-NADP-ME

WT	Forward 5'-GACTCCTATACC**TGG**CCTGAAGAAGCC-3' Reverse 5'-GGCTTCTTCAGG**CCA**GGTATAGGAGTC-3'
W572A	Forward 5'-GACTCCTATACC**GCG**CCTGAAGAAGCC-3' Reverse 5'-GGCTTCTTCAGG**CGC**GGTATAGGAGTC-3'
W572F	Forward 5'-GACTCCTATACC**TTC**CCTGAAGAAGCC-3' Reverse 5'-GGCTTCTTCAGG**TAA**GGTATAGGAGTC-3'
W572H	Forward 5'-GACTCCTATACC**CAC**CCTGAAGAAGCC-3' Reverse 5'-GGCTTCTTCAGG**GTG**GGTATAGGAGTC-3'
W572I	Forward 5'-GACTCCTATACC**ATC**CCTGAAGAAGCC-3' Reverse 5'-GGCTTCTTCAGG**GAT**GGTATAGGAGTC-3'
W572S	Forward 5'-GACTCCTATACC**TCC**CCTGAAGAAGCC-3' Reverse 5'-GGCTTCTTCAGG**GGA**GGTATAGGAGTC-3'

TABLE 2S
Kinetic parameters of the recombinant pigeon c-NADP-ME

	$K_{m,Mn}$ (μM)	$K_{m,Mal}$ (mM)	$K_{m,NADP}$ (μM)	k_{cat} (s^{-1})
WT	3.6 ± 0.1	0.10 ± 0.01	3.8 ± 0.5	225 ± 20
W572A	5.5 ± 0.3	0.14 ± 0.01	3.4 ± 0.5	246 ± 4
W572F	7.5 ± 1.3	0.25 ± 0.06	4.9 ± 1.1	224 ± 22
W572H	5.7 ± 0.1	0.12 ± 0.02	6.3 ± 1.3	222 ± 9
W572I	6.3 ± 0.7	0.14 ± 0.02	3.8 ± 0.6	247 ± 11
W572S	5.3 ± 0.4	0.13 ± 0.02	4.4 ± 0.7	266 ± 22

Table 3S
Thermostability of the recombinant pigeon c-NADP-ME

	± Mn^{2+} (4 mM)	T_m (˚C)
WT	-	57.7 ± 2.4
	+	60.5 ± 3.4
W572A	-	58.5 ± 2.3
	+	59.8 ± 2.9
W572F	-	57.2 ± 0.1
	+	59.1 ± 0.4
W572H	-	58.1 ± 2.3
	+	60.6 ± 2.7
W572I	-	57.4 ± 2.6
	+	59.1 ± 2.8
W572S	-	57.5 ± 2.7
	+	58.9 ± 2.8

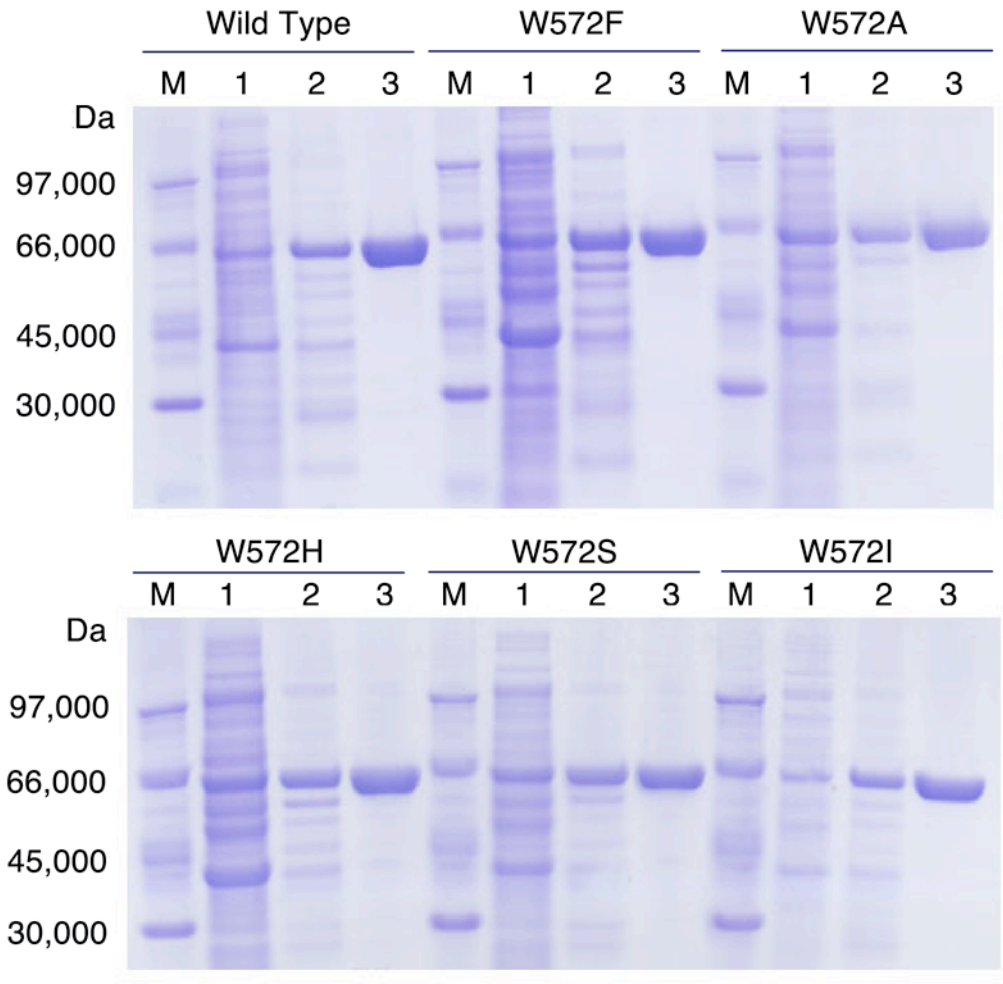

FIGURE 1S. **Polyacryamide gel electrophoresis of the recombinant pigeon c-NADP-ME in the presence of sodium dodecyl sulfate.** The enzymes eluted from two columns were analyzed by SDS-PAGE. Lane M, molecular weight standards: phosphorylase b (97 kDa), bovine serum albumin (66 kDa), ovalbumin (45 kDa), carbonic anhydrase (30 kDa). Lane 1, crude extract; Lane 2, eluent from Q-Sepharose. Lane 3, eluent from 2', 5'-ADP-Sepharose.

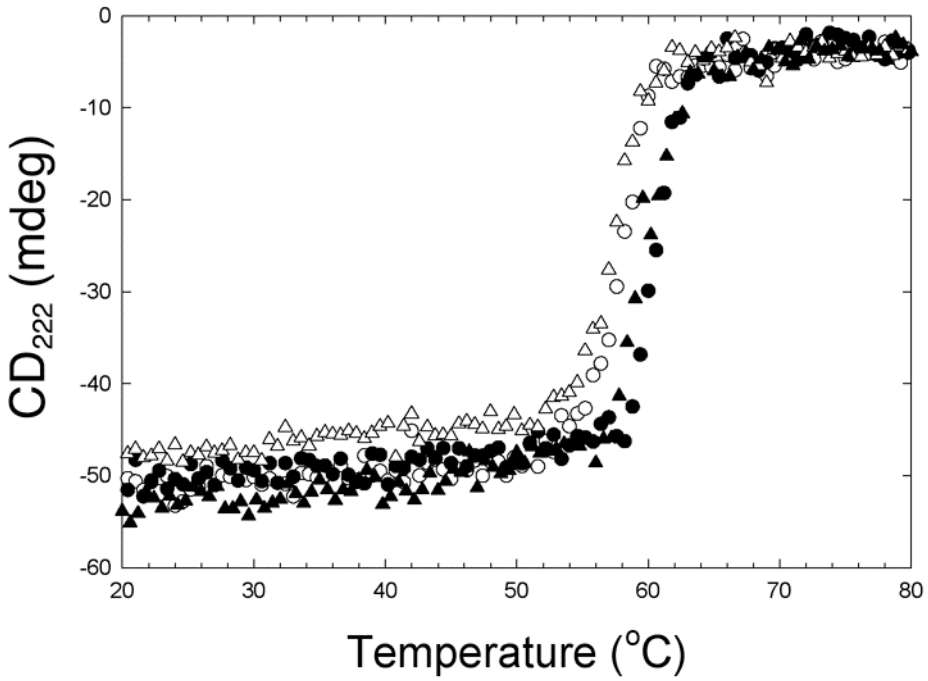

FIGURE 2S. **Thermal stability of the recombinant pigeon c-NADP-ME**. The CD at 222 nm of WT (circles) and W572F (triangles) c-NADP-ME in the absence (open) or in the presence of 4 mM Mn^{2+} (closed) were determined at a continuously elevating temperature. The concentration of protein was 0.4 mg/ml.

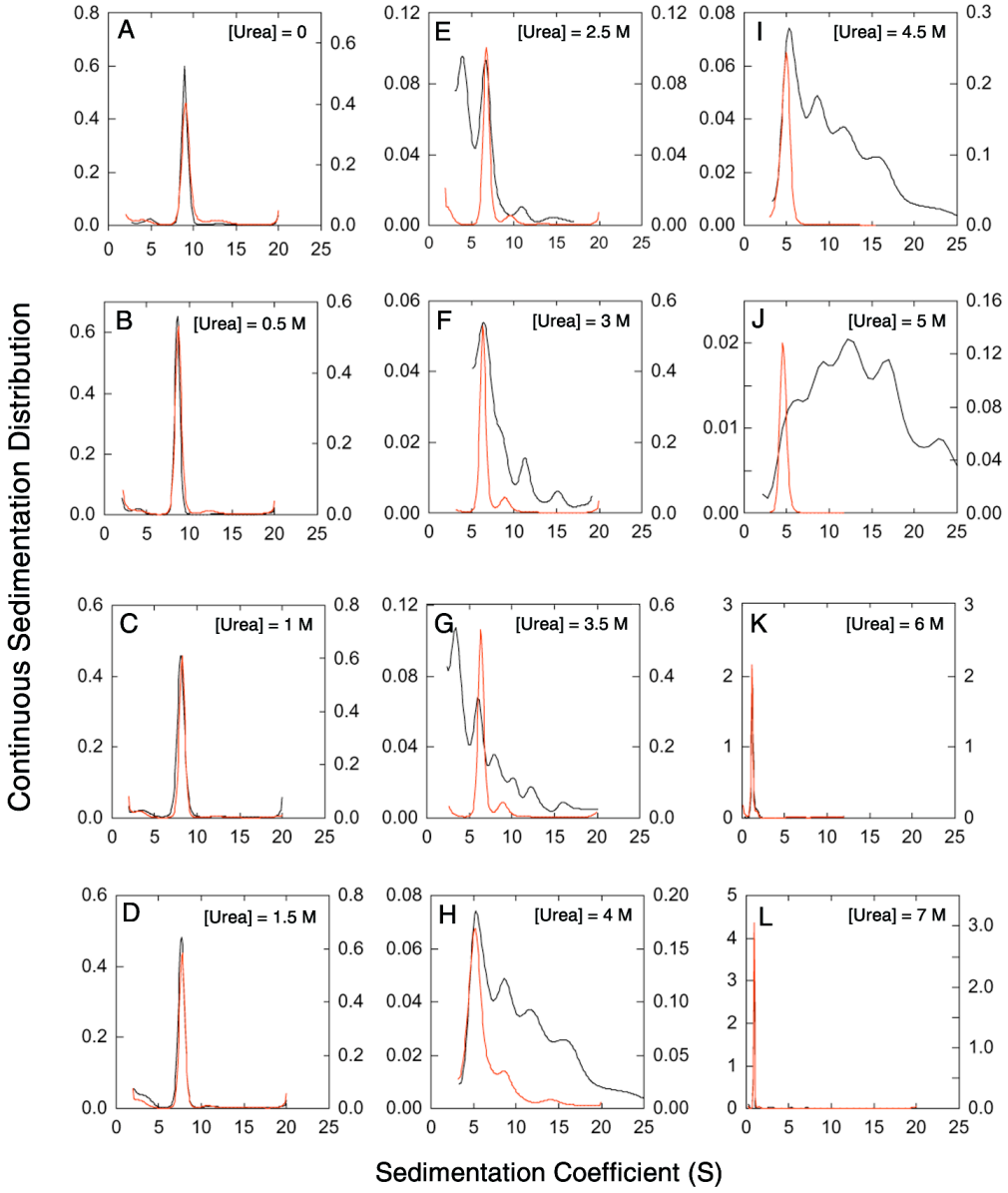

FIGURE 3S. **Effect of metal ion on the quaternary structure of pigeon c-NADP-ME**. Each panel represents the experimental results of unfolding the enzyme in different urea concentrations: (A) 0, (B) 0.5, (C) 1, (D) 1.5, (E) 2.5, (F) 3, (G) 3.5, (H) 4, (I) 4.5, (J) 5, (K) 6, and (L) 7 M. In all panels, the *black* (left scales) and *red* (right scales) lines represented the continuous sedimentation distribution of the enzyme unfolded with urea in absence and in the presence of 4 mM Mn^{2+}, respectively. Protection of the enzyme from aggregation is obvious at urea concentration of 4-5 M.

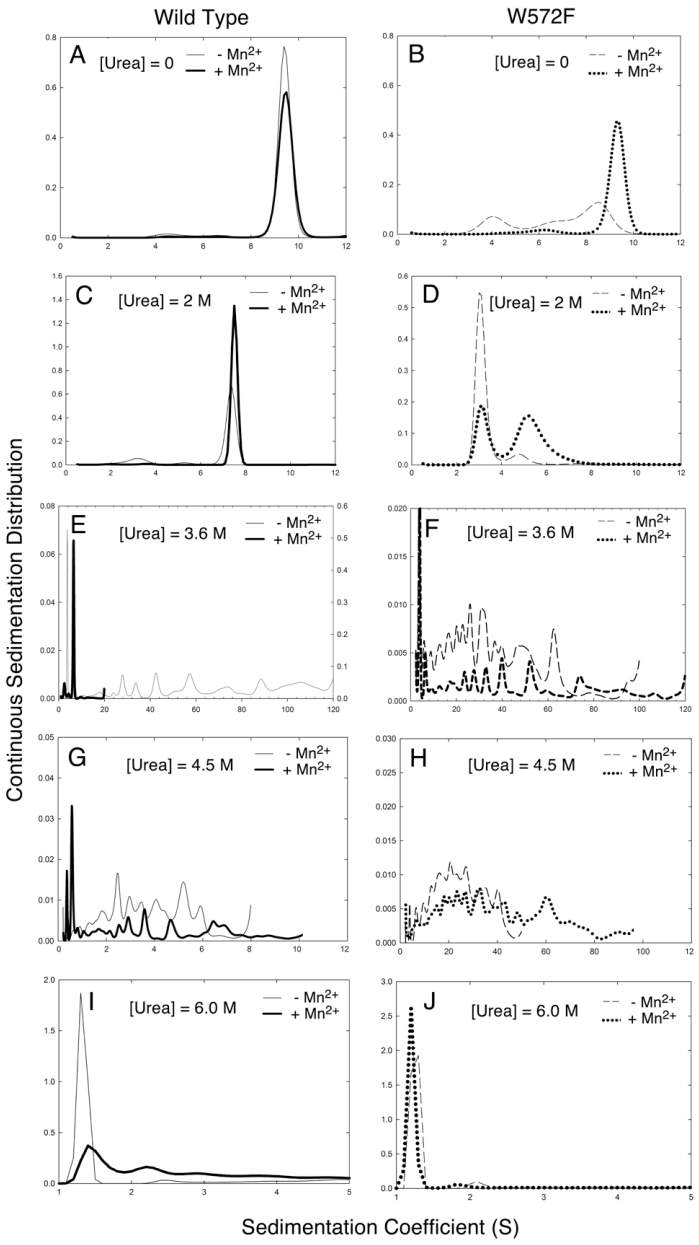

FIGURE 4S. **Sedimentation velocity patterns of WT and W572F pigeon c-NADP-ME in the presence or absence of Mn^{2+}.** The concentration of enzyme was 0.4 mg/ml in 100 mM Tris-acetate and incubated for 1 h at 25 ˚C. Each panel represented the continuous sedimentation distribution of the enzyme unfolded in different urea concentrations: (*A* and *B*) 0, (*C* and *D*) 2 M, (*E* and *F*) 3.6 M, (*G* and *H*) 4.5 M, (*I* and *J*) 6 M urea. (*A, C, E, G*, and *I*) WT, (*B, D, F, H*, and *J*) W572F. The c(s) signal of the WT enzyme with Mn^{2+} is on the right axis in *E*.

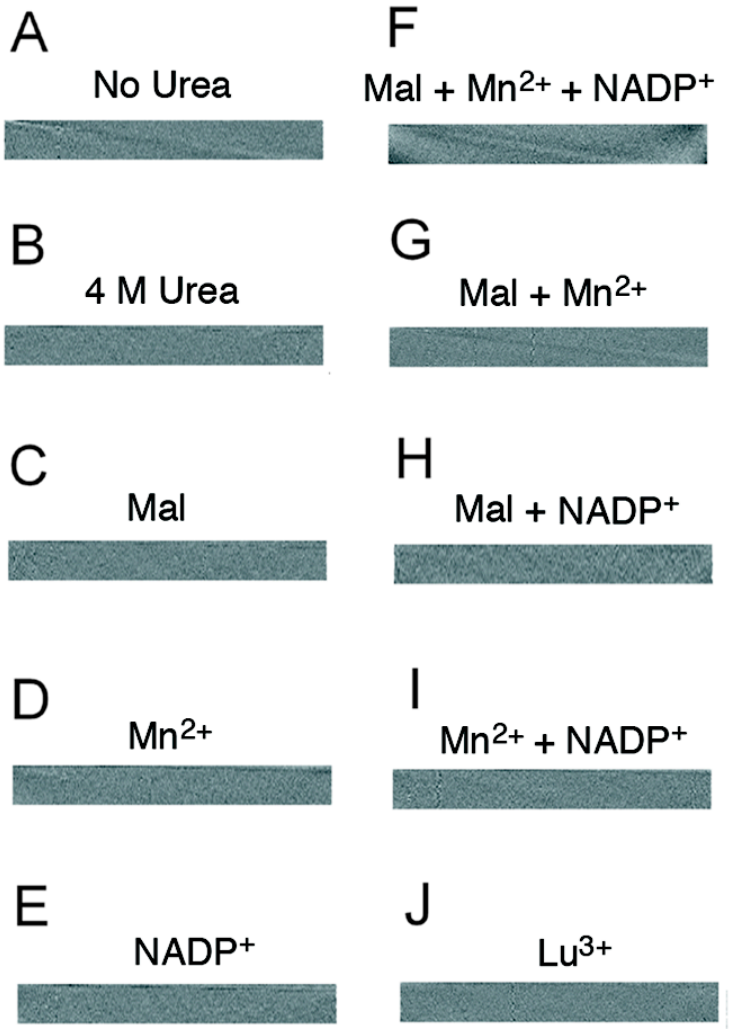

FIGURE 5S. **Fitting quality of the sedimentation data in the effect of ligands on the quaternary structure of malic enzyme during urea denaturation.** The homogeneous gray bitmaps indicate the reliability of AUC data fitting corresponding to Fig. 3 in the main text. *A*, Sedimentation velocity pattern of pigeon c-NADP-ME (0.75 mg/ml) in 30 mM Tris-acetate buffer, pH 7.4, contains 2 mM 2-mercaptoethanol. In *B*-*J*, Same concentration of c-NADP-ME was preincubated with: *B*, 30 mM Tris-acetate buffer/2 mM 2-mercaptoethanol (pH 7.4) only, no ligand added; *C*, 5 mM malate; *D*, 4 mM Mn^{2+}; *E*, 0.23 mM $NADP^{+}$; *F*, 5 mM malate, 4 mM Mn^{2+}, plus 0.23 mM $NADP^{+}$; *G*, 5 mM malate plus 4 mM Mn^{2+}; *H*, 5 mM malate plus 0.23 mM $NADP^{+}$; *I*, 4 mM Mn^{2+} plus 0.23 mM $NADP^{+}$; and *J*, 60 mM Lu^{3+}; and then treated with 4 M urea at 25 °C for 2-h.

A

MKKGYEVLRDPHLNKGMAFTLEERQQLNIHGLLPPCFLGQDAQVYSILKNFE
RLTSDLDRYILLMSLQDRNEKLFYKVLTSDIERFMPIVYTPTVGLACQHYGL
AFRRPRGLFITIHDRGHIATMLQSWPESVIKAIVVTDGERILGLGDLGCYGM
GIPVGKLALYTACGGVKPHQCLPVMLDVGTDNETLLKDPLYIGLRHKRIRGQ
AYDDLLDEFMEAVTSRYGMNCLIQFEDFANANAFRLLHKYRNKYCTFNDDIQ
GTASVAVAGLLAALRITKNRLSDHTVLFQGAGEAALGIANLIVMAMQKEGVS
KEEAIKRIWMVDSKGLIVKGRASLTPEKEHFAHEHCEMKNLEDIVKDIKPTV
LIGVAAIGGAFTQQILQDMAAFNKRPIIFALSNPTSKAECTAEQCYKYTEGR
GIFASGSPFDPVTLPSGQTLYPGQGNNSYVFPGVALGVISCGLKHIGDDVFL
TTAEVIAQEVSEENLQEGRLYPPLVTIQQVSLKIAVRIAKEAYRNNTASTYP
QPEDLEAFIRSQVYSTDYNCFVADSYTWPEEAMKVKL

B

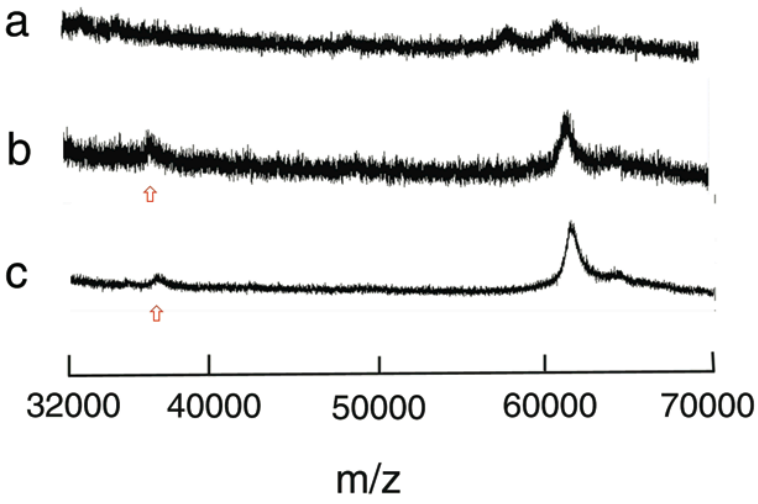

FIGURE 6S. **Identification of tryptic cleavage site of pigeon c-NADP-ME**. *A*, Amino acid sequence of c-NADP-ME. Arrows showed the putative trypsin cleavage site in the presence of Mn^{2+}. The N-terminal five amino acid sequence of the 37 kDa fragment (the bold type) was identified using an amino acid sequencing system. *B*, MALDI-TOF spectrum of malic enzyme in: (a), 30 mM Tris buffer/2 mM 2-mercaptoethanol (pH 7.4); (b), In the presence of 4 mM Mn^{2+}; and (c), in the presence of 5 mM malate plus 4 mM Mn^{2+}. The mass spectral changes in the samples shown in Fig. 5 were monitored for up to 3-h. Arrows showed the newly identified fragment of the final results.

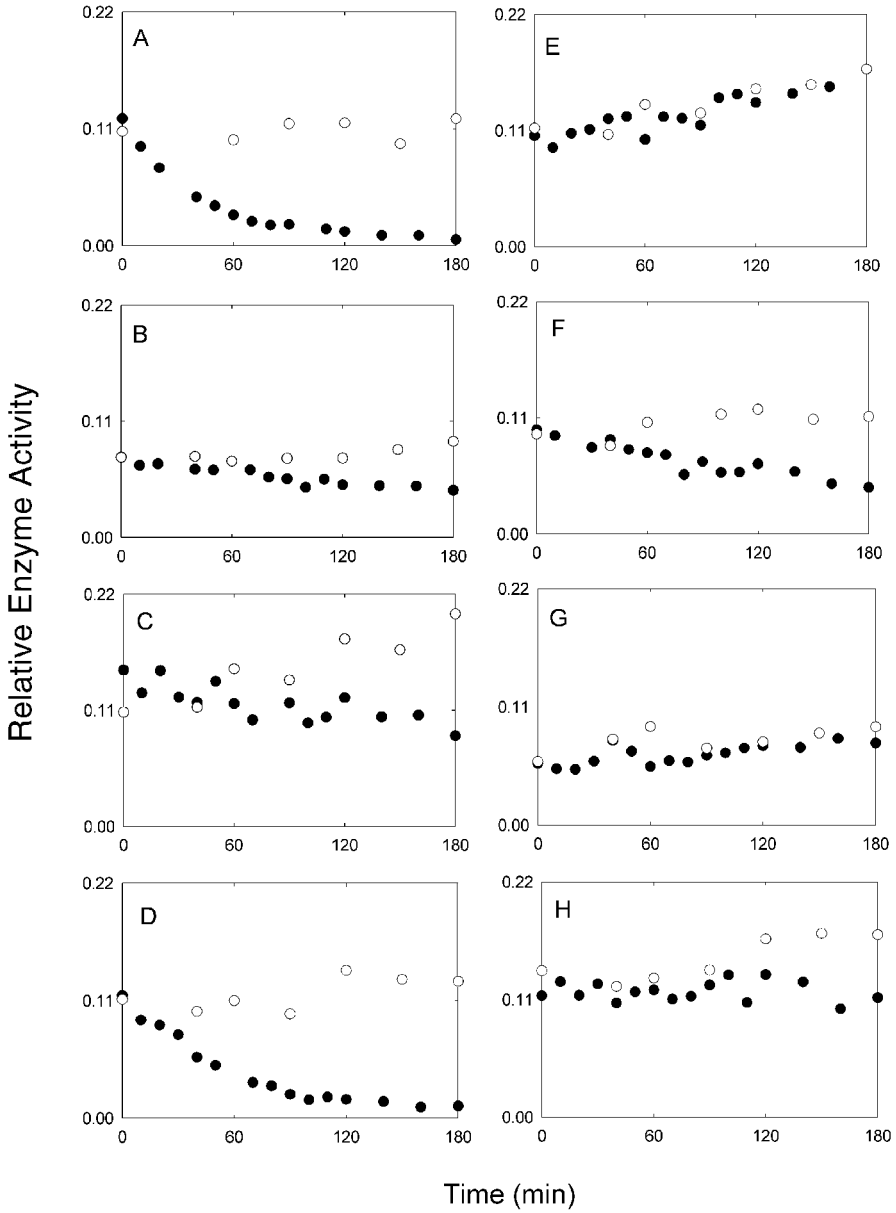

FIGURE 7S. **Effect of ligands on the inactivation of pigeon c-NADP-ME during tryptic digestion**. ME was preincubated with ligands and then treated with (closed circles) or without (open circles) trypsin. The slight increase in enzyme activity in all controls was due to an inevitable evaporation of sample volume after a long incubation time at 37 °C. *A*, no ligand; *B*, 5 mM malate; *C*, 4 mM Mn^{2+}; *D*, 0.23 mM $NADP^{+}$; *E*, 5 mM malate, 4 mM Mn^{2+}, plus 0.23 mM $NADP^{+}$; *F*, 5 mM malate plus 4 mM Mn^{2+}; *G*, 5 mM malate plus 0.23 mM $NADP^{+}$; *H*, 4 mM Mn^{2+} plus 0.23 mM $NADP^{+}$.

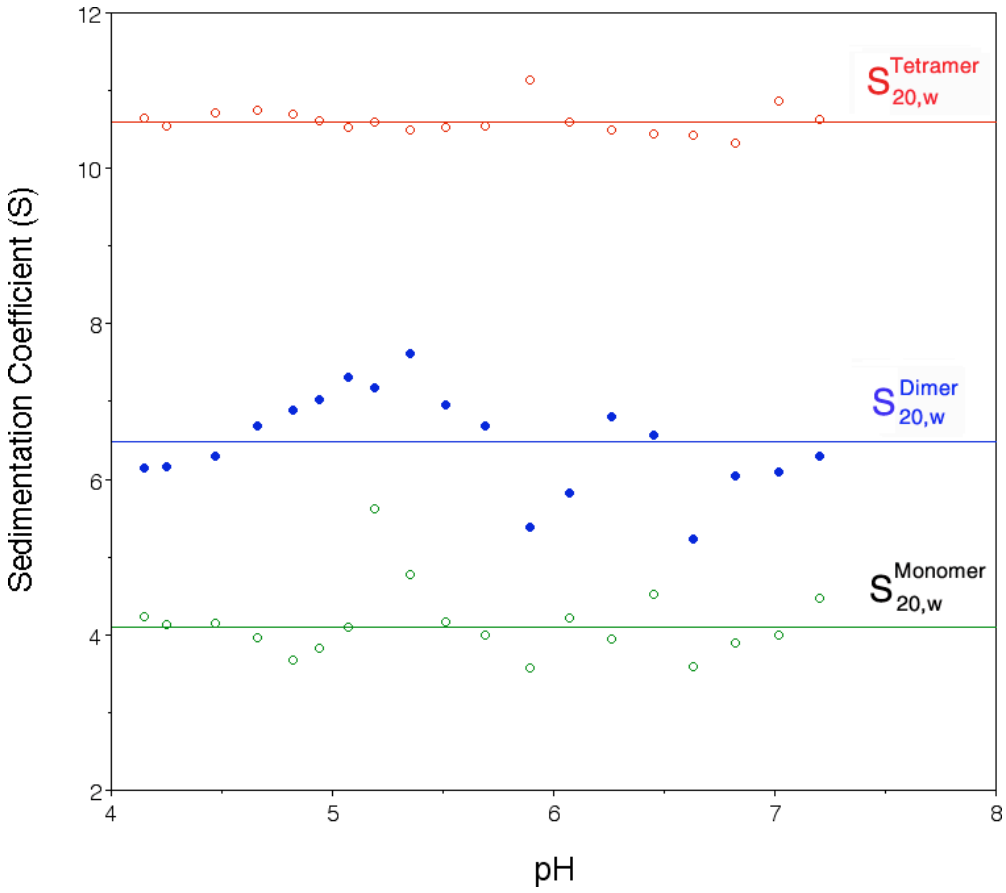

FIGURE 8S. **Sedimentation coefficient of the human m-NAD-ME.** m-NAD-ME sedimentation velocity experiments were performed at three protein concentrations (1 mg/ml, 0.3 mg/ml and 0.02 mg/ml) and at various pH values. The data were globally analyzed using the SEDPHAT program according to a monomer-dimer-tetramer model. The corrected sedimentation coefficient under standard conditions ($S_{20,W}$) and the equilibrium dissociation rate constants (k_{off}) (not shown in figure) of the tetramer-dimer-monomer system were found to be pH-independent.

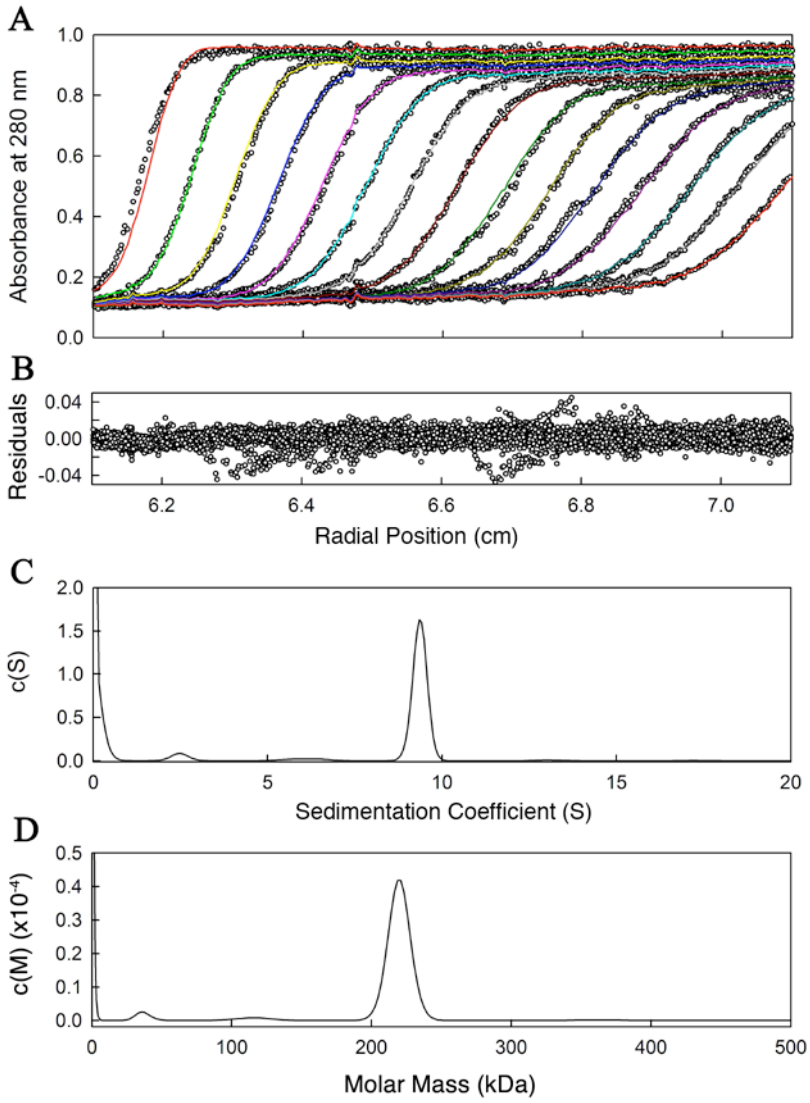

FIGURE 9S. **Sedimentation velocity analysis of the human m-NAD-ME at pH 7.02**. The enzyme concentration was 1.0 mg/ml. *A*, Trace of absorbance at 280 nm during sedimentation. For clarity, some of the spectra were omitted. *B*, Residuals of the model fitting. *C*, Continuous sedimentation coefficient distribution. *D*, Continuous molar mass distribution.

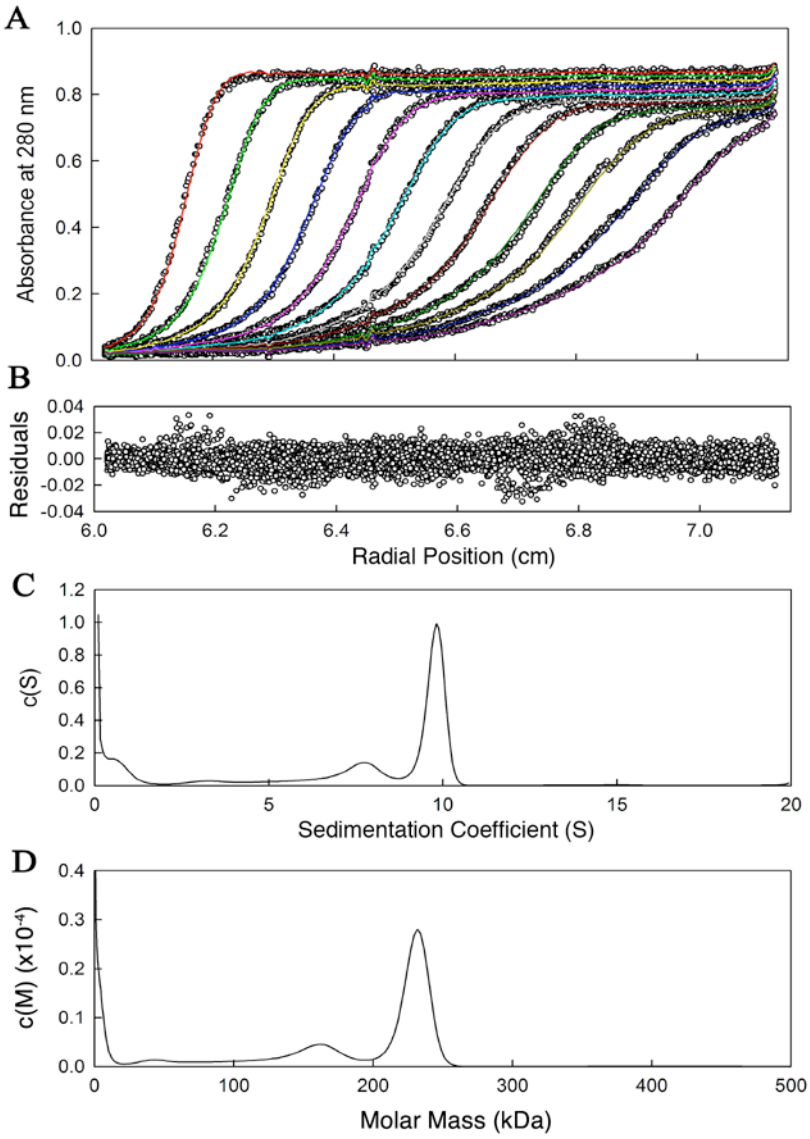

FIGURE 10S. **Sedimentation velocity analysis of the human m-NAD-ME at pH 5.19.** The enzyme concentration was 1.0 mg/ml. *A*, Trace of absorbance at 280 nm during sedimentation. For clarity, some of the spectra were omitted. *B*, Residuals of the model fitting. *C*, Continuous sedimentation coefficient distribution. *D*, Continuous molar mass distribution.

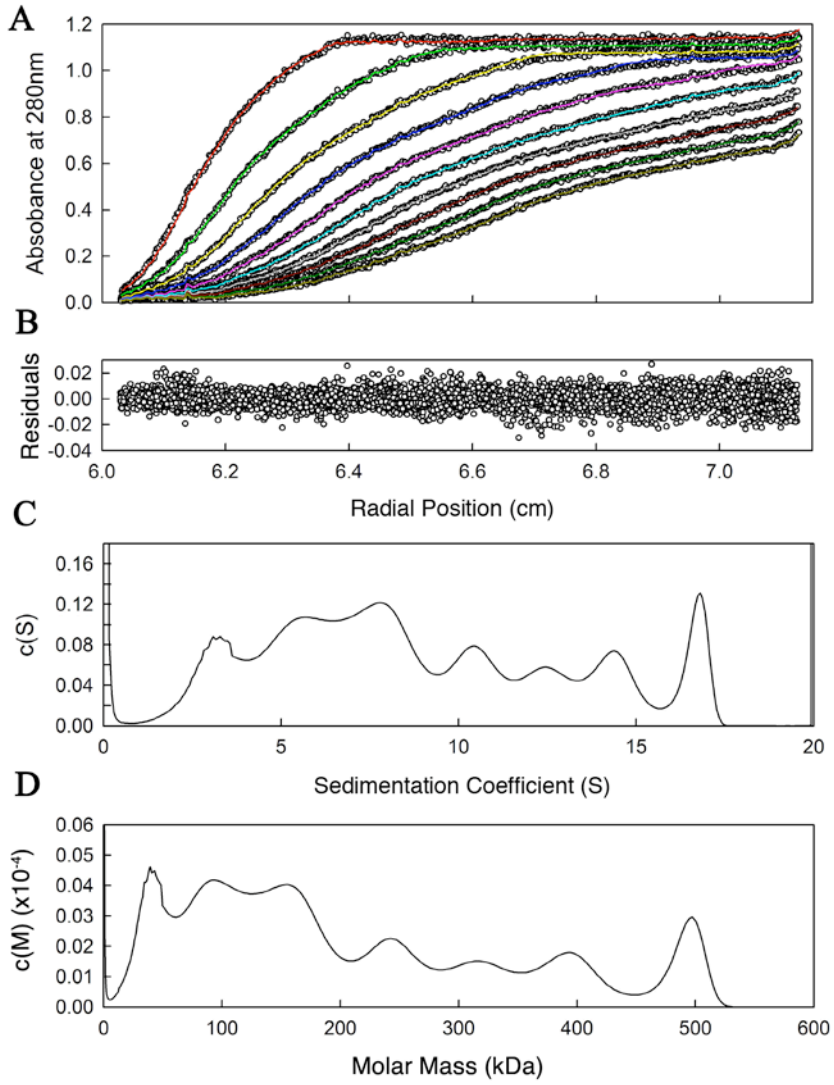

FIGURE 11S. **Sedimentation velocity analysis of the human m-NAD-ME at pH 3.88.** The enzyme concentration was 1.0 mg/ml. *A*, Trace of absorbance at 280 nm during sedimentation. For clarity, some of the spectra were omitted. *B*, Residuals of the model fitting. *C*, Continuous sedimentation coefficient distribution. *D*, Continuous molar mass distribution.

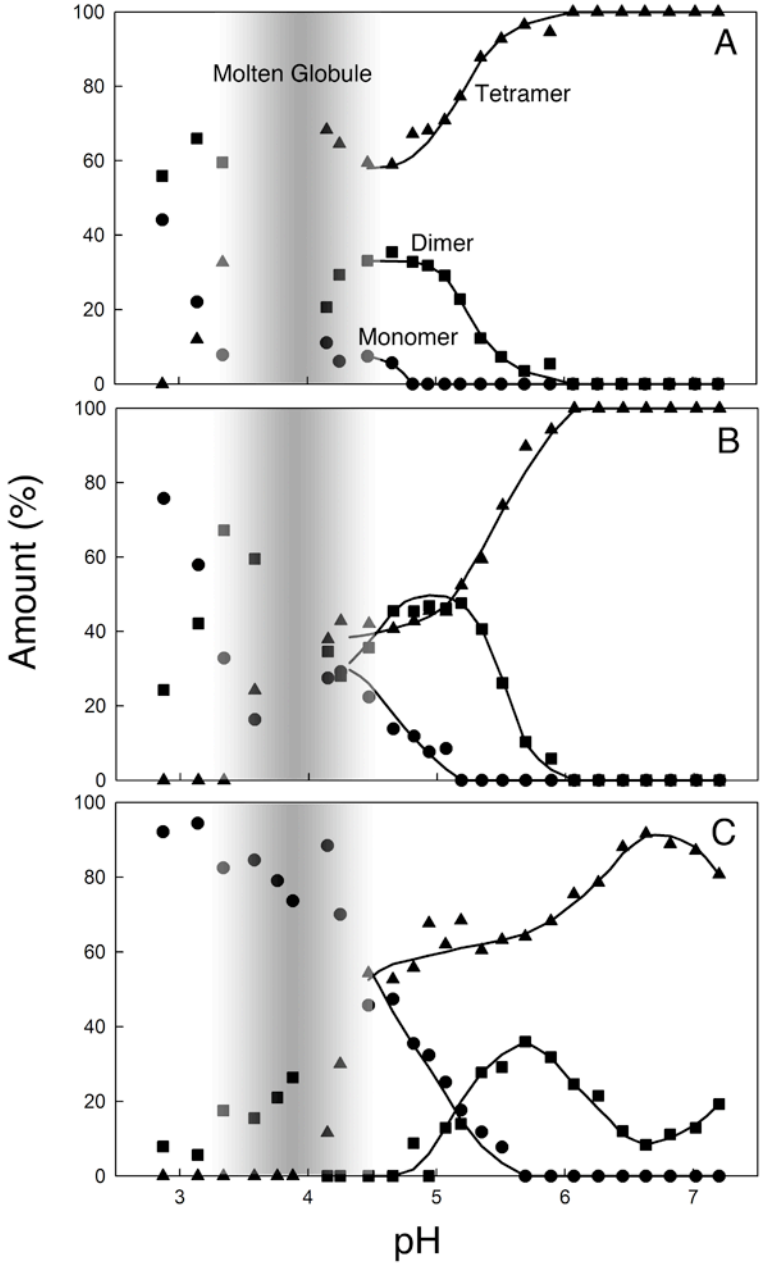

FIGURE 12S. **Acid-induced quaternary structural changes of the human m-NAD-ME.** The distribution of the quaternary structure was examined by AUC. The grey areas represented the enzyme existing in the putative molten globule state. The gradient roughly reflects the visible amount of precipitation. In the areas where agglutination was visible, no attempt was made to quantify each form. The protein concentrations were 1.0, 0.3 and 0.02 mg/ml, respectively, for panels *A, B* and *C*.

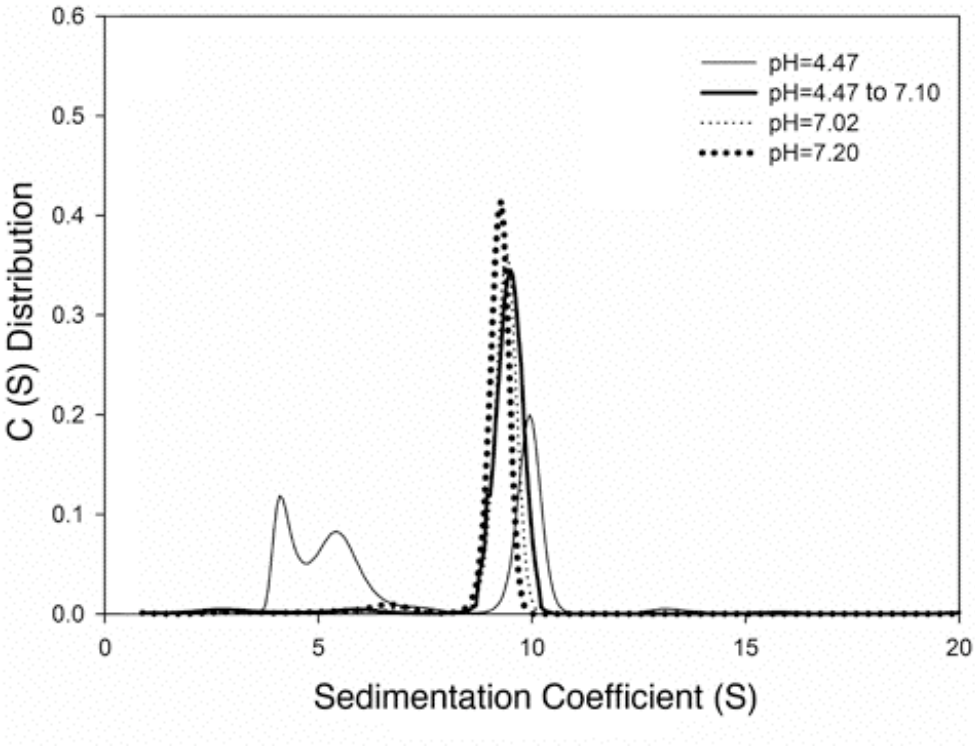

FIGURE 13S. **Reversibility of the acid-induced dissociation of the human m-NAD-ME.** The continuous sedimentation coefficient patterns of the enzyme (0.3 mg/ml) at pH 4.47 (thin line) and pH-jumped from 4.47 to 7.10 (bold line) demonstrate the reversibility of the quaternary structural changes. For comparison, the c(S) patterns of the enzyme at pH 7.02 (thin dots) and 7.20 (bold dots) are also shown.

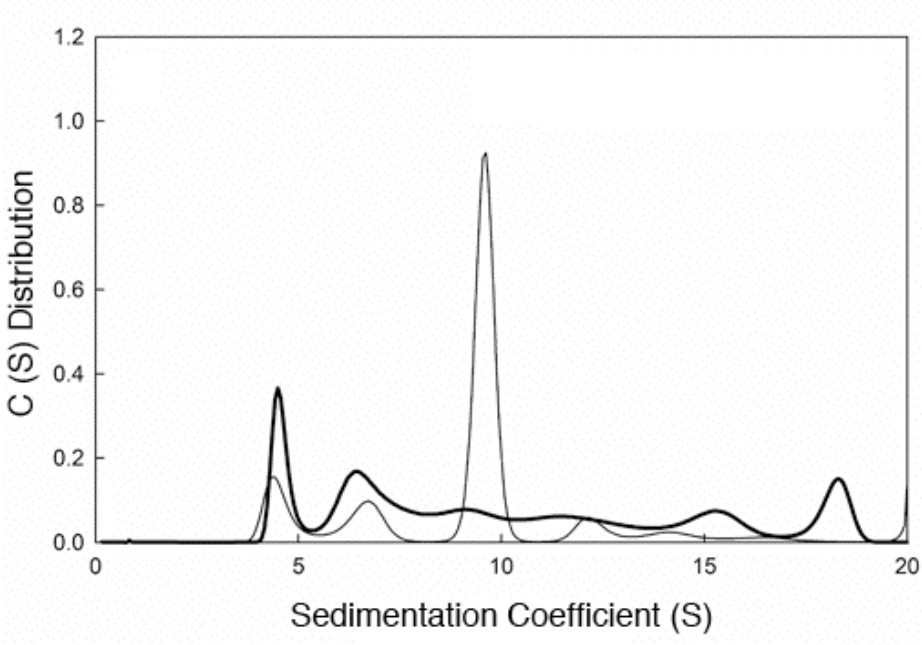

FIGURE 14S. **Protection against the acid-induced aggregation of the human m-NAD-ME by magnesium chloride.** Continuous sedimentation coefficient distribution of the enzyme (1 mg/ml) preincubated with metal ions (thin line, 20 mM; heavy line, 0.67 mM) and then pH jumped from 7.4 to 3.88.

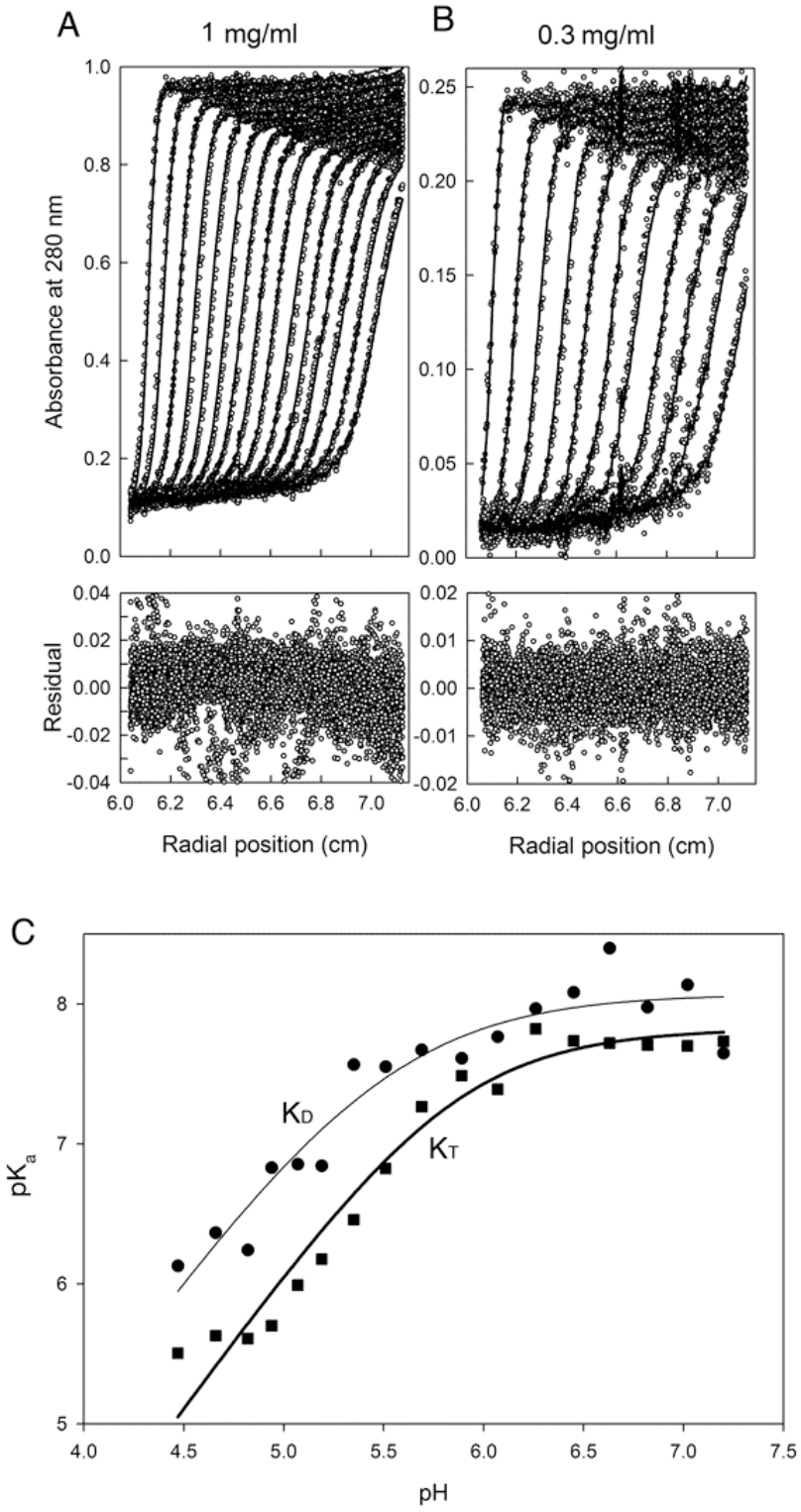

FIGURE 15S. **Tetramer-dimer-monomer equilibrium of the human m-NAD-ME.** (*A-B*), Typical sedimentation velocities of the enzyme at different protein concentrations. The circles are experimental data and the lines are global analysis of the data using the SEDPHAT program according to an equilibrium tetramer-dimer-monomer model.

$$Tetramer(T) \xleftrightarrow{K_T} 2Dimer(D) \xleftrightarrow{K_D} 4Monomer(M)$$

in which $K_T = \frac{[D]^2}{[T]}$, $K_D = \frac{[M]^2}{[D]}$, and the overall dissociation constant of tetramer to monomer is $K_{TD} = K_T \bullet K_D{}^2 = \frac{[M]^4}{[T]}$.

This was used to calculate the dissociation constants of the dimer interface (K_T) and tetramer interface (K_D). The fitting residuals are shown under each panel. The local root mean square error values are between 0.0076 and 0.0136. *C*, Correlation of K_T and K_D with pH. The lines represent the fitting results of the dissociation constants K_T and K_D according to the following pH dependence of pK_a function

$$\log K_a = \log\left(\frac{C}{1 + \frac{[H^+]}{K_1} + \frac{[H^+]^2}{K_1 K_2}}\right)$$

in which K_a is the observed dissociation constant measured by AUC at any pH, *C* is the pH independent value of K_a, $[H^+]$ is the proton concentration and K_1 and K_2 represent the dissociation constants of the enzyme molecular groups. The data are best described by the involvement of two molecular groups with pK_a values of 6.0 ± 0.4 and 5.7 ± 0.4 on the dimer interface and 5.8 ± 0.3 and 5.2 ± 0.4 on the tetramer interface, respectively, for the tetramer-dimer and dimer-monomer processes.

On examining the interfacial regions, no salt bridge between any of the interfacial regions was found. Other ionizable groups, including His-142, His-125, Asp-139 and Asp-568, are likely to be the groups responsible for the pK_a values detected by AUC. Previously, we have discovered Trp-572 to be a critical residue involved in the quaternary stability of the c-NADP-ME (12,13). It would be interesting to discover the relationship between Trp-572 and the other interfacial ionizable groups and this might provide insights into the intriguing control process of the ME quaternary structure stability.